FCT
Fundação para a Ciência e a Tecnologia
MINISTÉRIO DA CIÊNCIA, TECNOLOGIA E ENSINO SUPERIOR

COMPETE
PROGRAMA OPERACIONAL FACTORES DE COMPETITIVIDADE

FCT PROJECT P2020-PTDC/ECM-EST/1056/2014 –

"IntegraCrete – A comprehensive multi-physics and multi-scale approach to the combined effects of applied loads and thermal/shrinkage deformations in reinforced concrete structures"

Prediction of thermal properties of concrete material at early ages using a multiscale modelling strategy

Task 2 – Bridging scales of analysis: from micro to macro

Authors:

Hadi Mazaheripour, Rui Faria, Miguel Azenha, Amin Abrishambaf, Guang Ye

Faculdade de Engenharia da Universidade do Porto (FEUP), 2018

1. Introduction

Prediction of the thermomechanical behaviour of concrete depends on the adequate knowledge of its thermal properties. Specific heat capacity, thermal conductivity and the coefficient of thermal expansion (CTE) are the properties that play important roles in the structural behaviour of concrete structures (RC) at early ages, especially the massive ones [1], which are particularly prone to significant thermal stress development. At early ages, these thermal properties evolve with the changes in the microstructure, due to the cement hydration processes. Therefore, an understanding of the thermal properties of cement paste can contribute to the prediction of such properties for concrete. The evolution of thermal properties in concrete is strongly dependent on the change in the thermal properties of cement paste during hydration, which is mainly due to the difference between the thermal properties of the hydration product (i.e. Calcium-Silicate-Hydrate (C-S-H)) and those of the corresponding reactants. Therefore, understanding and modelling of the cement paste hydration process should be the first step in the modelling of the thermal properties of cement-based materials like concrete, especially at early ages.

The thermal properties of concrete depend on three different aspects including environmental, structural and compositional aspects [2]. In case of environmental aspects, temperature and moisture are the main parameters, which all the thermal properties are dependent on [3-5]. As a structural aspect, morphology of concrete material at different length scales has also influence on its physical and mechanical behaviour. For instance, crystals show a higher thermal conductivity rather than disordered and highly porous medium like concrete material [6]. Clinker composition, water-to-cement (w/c) ratio, the existence of supplementary cementitious materials (SCM) and the type of aggregates are also effective factors that are counted as compositional aspects [4, 7, 8].

The main contribution of the present work is to combine a numerical homogenization technique with hydration kinetics of cement paste, accounting to the structural and compositional aspects in order to estimate the thermal properties of concrete material. In this technical report, a multiscale numerical modelling strategy is proposed to estimate the thermal properties of concrete from early ages in respect with the change in the volume fraction of the cement paste hydration kinetics. The thermal properties of concrete are addressed by simulating the concrete material at four different scales: nano, micro, meso and macroscale. At each scale, a cubic Representative Elementary

Volume (REV) with a periodic boundary condition is considered for the modelling. The numerical platform is presented and described. The computational model was validated using some experimental data gathered from the literature. Finally, with the aid of the proposed numerical platform, a parametric study is carried out to evaluate the effect on the thermal properties of concrete of: (i) w/c; (ii) humidity (percentage of water content in porosity); (iii) variation of cement paste properties, and (iv) Interfacial Transition Zone (ITZ).

2. Materials, properties and mix design

This study focuses on CEM II 42.5R, as marketed in Portugal. The mineral composition of this cement was measured by means of a powder X-Ray Diffraction (XRD) technique. The obtained mass percentage of the cement is given in Table 1.

Table 1. Mineral composition of the cement obtained from XRD analysis

Components	C3S	C2S	C3A	C4AF	Quartz	Gypsum	Limestone	Anhydrite
Phase concentration (%)	63.2	2.6	7.6	11.6	0.5	1.7	11.3	1.4

Cement notation: C3S-Tricalcium Silicate; C2S-Dicalcium Silicate; C3A-Tricalcium Aluminate; C4AF-Calcium Iron Aluminium Oxide; Calcium Carbonate-limestone.

The cumulative particle size distribution (PSD) of cement was measured by using Laser Diffraction Spectrometry (LDS). In order to obtain the PSD curve of cement clinker itself, a PSD curve of limestone, as a typical SCM, was extracted from the obtained PSD curve for the cement. These two curves are plotted in Figure 1. The PSD curves can be fairly defined as a Rosin-Rammler function, i.e., $f(D)=1-e^{-b.D^n}$, where D is the diameter of the cement particle, and b and n are coefficients. By employing a curve fitting analysis, the values of 0.052 and 1.00 were calculated for cement clinker, and values of 0.16 and 2.0 for limestone, for respectively, b and n. These values will be used later for construction of the cement paste microstructure.

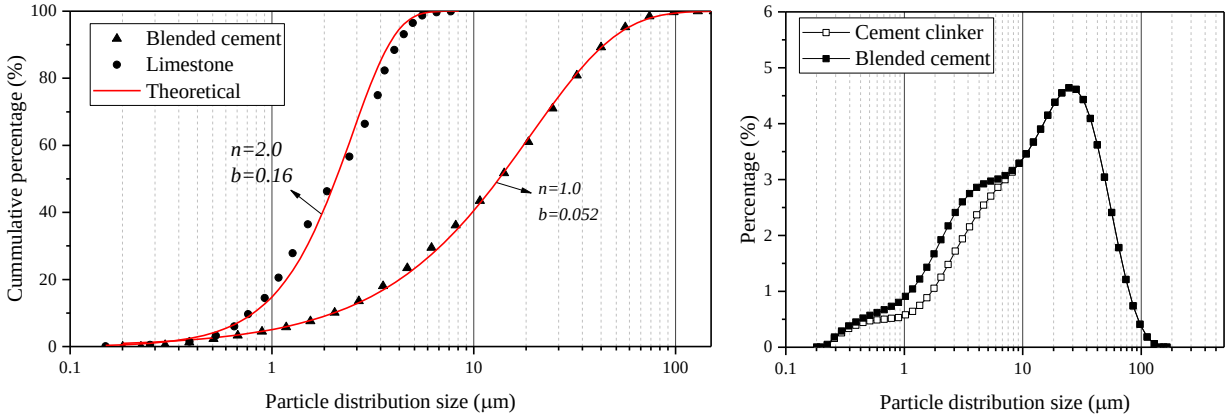

Figure 1. Particle distribution size of cement paste including limestone, and theoretical curves for cement clinker and limestone separately

Additionally, the particle size determination of the aggregates is plotted in Figure 2. The respective fitting curves are also shown in this figure, where the values of b and n are, respectively, 0.005 and 2.1 for coarse aggregates and 0.15 and 0.95 for sand aggregates. These values will be used later for construction of the mesoscale and macroscale structure of mortar and concrete.

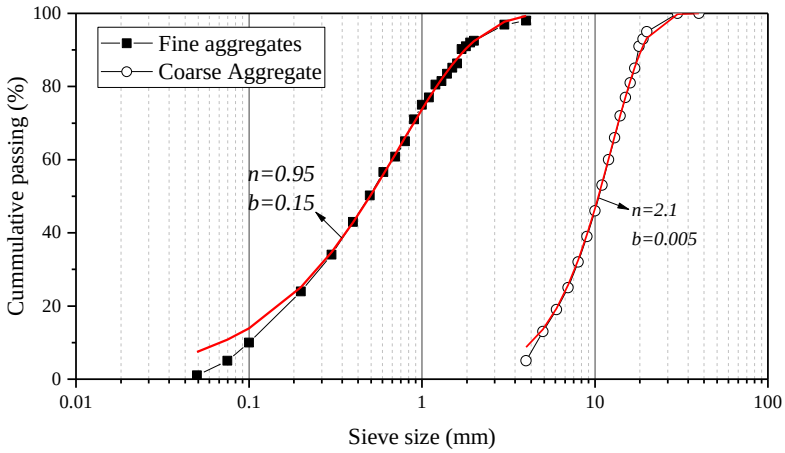

Figure 2. Particle distribution size of sand and coarse aggregates and the respective theoretical fitting curves

Despite the importance of the thermal properties of concrete at early ages, there are a few studies in the literature regarding the experimental measurement for the thermal properties of the fundamental phases, such as the hydration products. Based on the reported values in the literature, typical values of the thermal properties of the main individual components of concrete

material are summarized in Table 2, which are used in the modelling in the present study. These values correspond to a temperature around 20℃.

Table 2. Thermal properties of concrete components for the simulation in the present study

		Thermal conductivity λ	Specific heat capacity C_P	Thermal expansion coefficient (Volumetric)	Density ρ
		W/m.K	J/(kg.K)	$\alpha_T \times 10^{-6}$ (1/K)	g/cm^3
Clinker	C3S	3.45 [9]	0.69 [9]	49.5 [9]	3.13 [9]
	C2S	3.35 [9]	0.68 [9]	49.9 [9]	3.31 [9]
	Average	3.29	0.73	49.6	3.15
Limestone (saturated)		2.95 [10]	0.92 [10]	24 [10]	2.50 [10]
CH		1.32 [9]	1.15 [9]	99.1 [9]	2.17 [9]
C-S-H globules (Ca/Si=1.75)		0.98 [9]	0.84 [9]	45.0 [9]	2.6 [9]
HD C-S-H – saturated *		0.870 [9] (0.883)	0.86-0.97 [9] (0.88)	- (45.39)	- (2.18)
LD C-S-H– saturated *		0.825 [9] (0.830)	0.86-0.97 [9] (0.90)	- (54.12)	- (1.99)
Water in gel pores		0.607 [11]	1.13 [12]	356 [9]	1.0
Water in capillary pores		0.607 [11]	4.18	200 [9]	1.0
Aggregate (saturated)		3.15 [13]	845 [4]	0.4-10.2** [13]	2.65

* The values in the parenthesis obtained from the nanostructure model in the present study (see section 3.1).
** The value of 5×10^{-6} is adopted in the present study.

Difficulties in measuring the properties (particularly at early ages) are challenging, as it is reported in the literature [4] - for example moisture affects the properties since they are all moisture dependent. This is a reason to the importance of multiscale-based modelling strategies to estimate the thermal properties. Recently, an effort is made to determine the thermal properties of some hydration products through an atomic modelling level combined with statistical physics and a mean-field homogenization theory to determine the thermal properties of some hydration products [9]. Most of the values reported in Table 2 for hydration products have been taken from this recent study, as cited in the table.

To establish a multiscale pattern for theoretical estimation of the concrete properties, a concrete mix design is necessary to determine the volume percentage of the components. The adopted mix design in the present study is the one used in the IntegraCrete research project. The water to cement ration is w/c=0.62. The mass weight of the components in a unit cube meter of concrete

are given in Table 3. Based on the theoretical density adopted for each component, the corresponding theoretical volume is calculated. These values will be used to construct the structure of the cement paste, mortar and concrete in the following section.

Table 3. Concrete mix design and the calculated volume of its components for w/c=0.62

	Cement	water	Superplasticizer	Aggregates	
				Sand	Coarse
Practical mix composition (kg)	290	180	2.32	969	928
Theoretical density (g/cm^3)	3.15	1.0	1.18	2.65	
Theoretical volume (m^3)	0.09	0.18	0.002	0.366	0.35

3. Numerical strategy to estimate thermal properties

In this section, the numerical approach to estimate the thermal properties of concrete including the thermal expansion coefficient, the specific heat capacity and the thermal conductivity is described. The analysis at each length scale is implemented on a Representative Elementary Volume (REV). The material phases in REV are simulated by locating randomly the spherical particles. In case of the cement paste microstructure, the sphere is a cement particle, for mortar mesostructure is a sand particle, and for concrete macrostructure is the random parking of coarse aggregates. The details for REVs at each length scale are given later in the next sections. The construction of the REVs was made by employing the HYMOSTRUC3D computer software, which is mainly developed for modelling of hydration kinetics of cement paste [14, 15]. The software uses the vector approach for presenting the spherical geometry [16], therefore, the obtained REV has to be discretized in order to be used for the numerical modelling purpose. A computer code has been developed in the context of IntegraCrete project to establish an interface between the output results from HYMOSTRUC3D and a Finite Element Analysis (FEA) software, which is FEA DIANA software [17]. The REVs are discretized with $1x10^6$ smaller cubic voxels of 0.01 unit length, meaning that each length of REV is divided into 100 voxels. A single material phase is assigned for each voxel, based on the greatest volume fraction of the material that the voxel is representing in the original REV. For example, if the voxel is in the boundary of two material phases (e.g. inner and outer C-S-H in cement paste microstructure), the voxel represents the material with the higher

volume fraction. Each voxel represents a solid finite element. However, no element is assigned to the voxel representing air, empty space or pores, unless the latter are filled with water.

3.1. Thermal conductivity

The voxels of the discretised REV are considered as eight-node isoparametric solid finite elements, for a 3D potential flow analysis. Unit degree of temperature difference is imposed at two sides of the REV as shown in Figure 3, and it is numerically solved under a steady state heat transfer analysis. The effective thermal conductivity is calculated by

$$\lambda_{eff} = -\langle \Delta q_z \rangle L \tag{1}$$

where Δq_z is the average heat flux in the plane distanced z, as shown in Figure 3, derived by

$$\Delta q_z = \langle q_z^r \rangle \tag{2}$$

where q_z^r is the heat flux flowing through phase r in the plane z obtained from the output results of DIANA FEA. The operator $\langle . \rangle$ denotes volume averaging. The value L is the length of the REV in correspondence to the distance between the two opposite surfaces with a unit degree of temperature difference ($\Delta T = T_2 - T_1 = 1.0$).

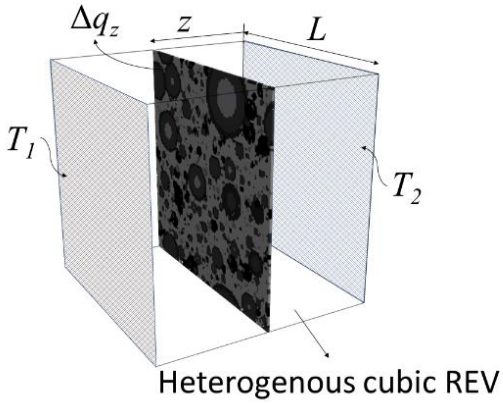

Figure 3. Schematic view of numerical calculation of the thermal conductivity on a heterogeneous cubic REV

3.2. Specific heat capacity

According to the thermo-elasticity, the elastic properties, the heat capacity, and the thermal expansion coefficient are correlated [2]. However, the contribution of heat energy to its elastic

behaviour can be neglected for cement-based material, meaning that the specific heat at constant volume (C_v) can be assumed as equal to the specific heat capacity per unit volume (C_p) [2, 9]. Therefore, the effective heat capacity per unit volume (C_p^{eff}) can be derived by

$$C_p^{eff} = \left\langle C_p^r \right\rangle \approx C_v^{eff} \tag{3}$$

where C_p^r is the specific heat capacity of phase r in the REV. The same calculation can be made to estimate the effective density of the REV, deriving by

$$\rho_{eff} = \left\langle \rho^r \right\rangle \tag{4}$$

where ρ^r is the density of phase r in the REV.

3.3. Coefficient of thermal expansion

The thermal expansion can be defined in terms of a scalar volumetric CTE, being the ratio between the volume change within a volume V and the temperature change in the absence of traction in the boundary ∂V [2, 18] (which means that the stresses are assumed as zero):

$$\left(\alpha_T\right)_v = \left(\frac{1}{V}\frac{\partial V}{\partial T}\right) \tag{5}$$

and for an isotropic medium, the scalar volumetric CTE is the triple of the linear scalar CTE:

$$\left(\alpha_T\right)_v = 3\left(\alpha_T\right)_L \tag{6}$$

If the temperature increases for a unit degree, then

$$\left(\alpha_T\right)_v = \left(\frac{\Delta V}{V}\right) \tag{7}$$

where the value of ΔV is the change in the volume of REV for a unit degree of temperature difference in all phases. To obtained this volume change, the discretized REV is imported to DIANA FEA software. The voxels are considered as eight-node isoparametric solid elements [17]. The displacements along x, y and z directions are fixed, respectively, at the nodes located at the REV square faces with $x = 0$, $y = 0$ and $z = 0$. Based on this configuration, the volumetric change of the REV is similar to the schematic illustration in Figure 4. The temperature of all elements increased for a unit degree in respect with the initial temperature, and the model is

solved under a linear elastic analysis. According to the displacement field obtained for all the nodes, ΔV is derived by

$$\Delta V = V - \left(L + \bar{\Delta}_x\right)\left(L + \bar{\Delta}_y\right)\left(L + \bar{\Delta}_z\right) \tag{8}$$

with

$$V = L^3 \tag{9}$$

and $\bar{\Delta}_x$, $\bar{\Delta}_y$ and $\bar{\Delta}_z$ are the average displacements of the nodes located, respectively, at the REV square faces with $x = L$, $y = L$ and $z = L$. The linear scalar CTE can be derived along each direction by

$$\left(\alpha_T\right)_L = \frac{\bar{\Delta}}{L} \tag{10}$$

Both linear and volumetric results of CTE are presented later for the REVs at different modelling scales.

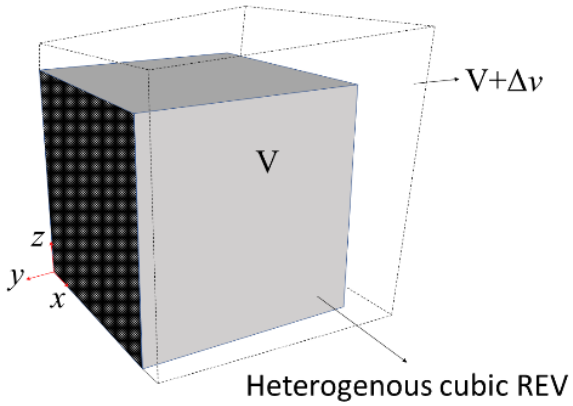

Figure 4. Schematic view of volume change in a heterogeneous cubic REV with a unit degree of temperature difference with respect to the initial temperature

4. Multiscale definition of concrete

The heterogeneity of cement-based materials demonstrates itself at different length scales. In order to develop an appropriate multiscale modelling scheme, it is essential to consider the spatial and temporal scales involved, and how the physical processes and characteristics of the system associate with the corresponding scale [19]. A careful definition of relevant length scales can clarify any investigation of scale considerations, although such definitions are a matter of choice and modelling approach [20]. In general, the length scale in cement-based systems may vary

from a nano-level in the order of 10^{-9}m to a macro-level on the order of 1m for some regional applications. A scale grade in cement-based materials is defined and illustrated in Figure 5, which consist of four fundamental levels, i.e., nanoscale (gel pore scale), microscale (capillary pore scale), mesoscale (cement paste and fine aggregates) and macroscale (mortar and coarse aggregates).

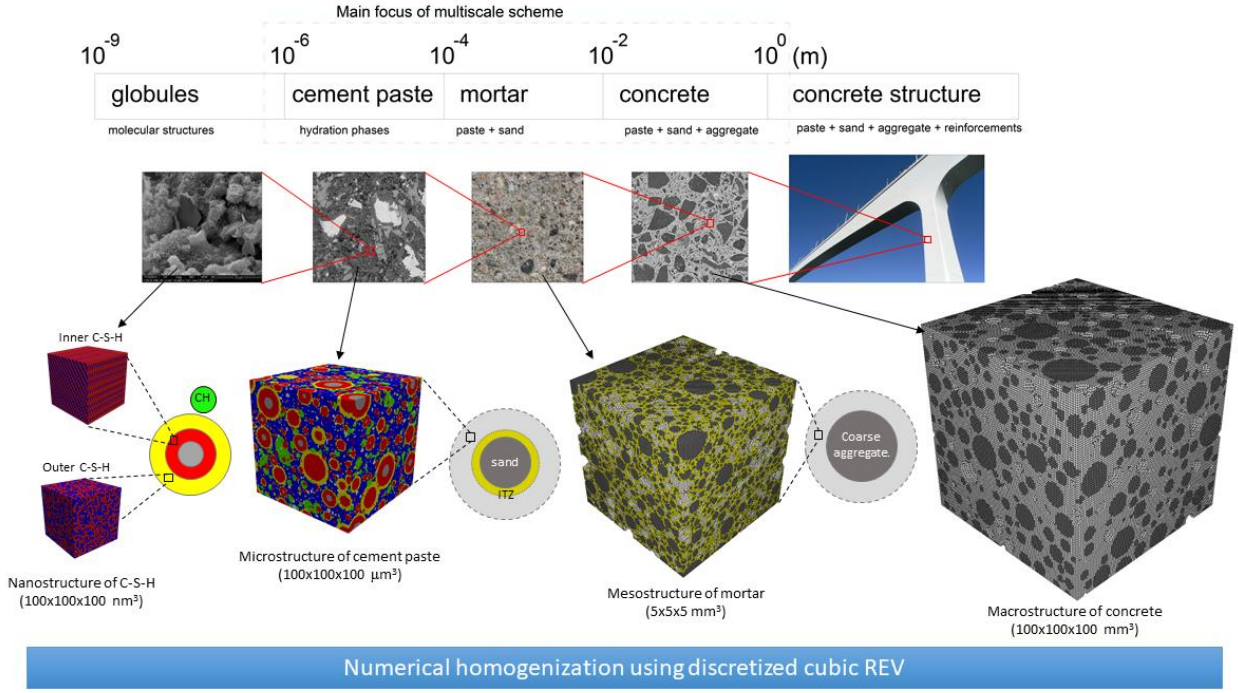

Figure 5. Definition of different modelling scales in cement-based materials

4.1. Nanoscale

Nanoscale refers to the nanostructure of the main hydration product Calcium-Silicate-Hydrate (C-S-H). According to the literature, the C-S-H product forms as high- and low-dense shape, the former called HD C-S-H and the later LD C-S-H. The REV nanostructure of LD C-S-H is constructed by assuming the random close packing of mono-sized (5nm) C-S-H sphere globules (Figure 6 - left). The random close packing of mono-sized is equivalent to "*the maximum density that a large, random collection of spheres can attain, and this density is a universal quantity*" [21]. This packing density of mono-sized sphere is about 0.64, which is very close to the packing density reported for the LD C-S-H globules [9]. In this study, the code from Skoge *et al.* [22] is used to generate the nanostructure of outer C-S-H, which is based on a molecular dynamics

mechanism. The REV nanostructure of the HD C-S-H is also simulated by the close packing of mono-sized (5nm) C-S-H globules (Figure 6 - right). For the case of the HD C-S-H, the close packing of mono-sized spheres is arranged in a lattice, and not as a random form. The packing density is approximately 0.74, which is higher than that of the random close packing, and it is very close to the density reported for the HD C-S-H in the literature [9].

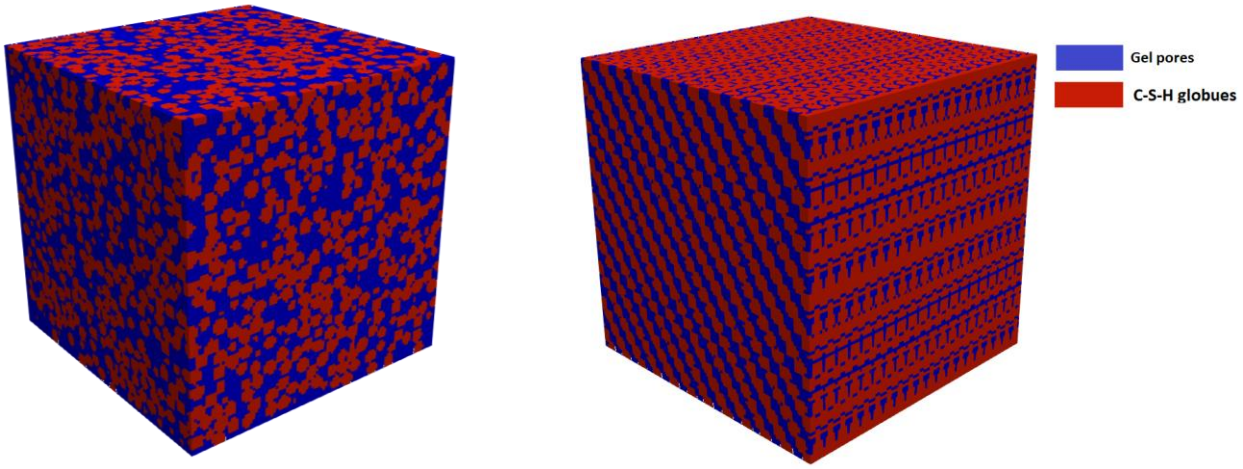

Figure 6. Nanostructure of the LD C-S-H (left) and the HD C-S-H (right) hydration product in cement paste

The discretised REV nanostructures of C-S-H are solved in DIANA FEA under a steady state heat transfer analysis and a linear structural analysis as described in Section 3. The results from these two analyses are shown in Figure 7 for only the LD C-S-H example. The left side figure shows the heat flux along direction z, while the right-side figure shows the maximum deformation field of the REV among all the three directions, as an output of the linear elastic analysis for a unit temperature variation. By using Eq. (1), the effective thermal conductivity can be obtained. Note that the length size of the elements in FE model are arbitrary chosen unitary (1m), however, it represents 1nm in a real scale of C-S-H. By using Eqs. (7) and (10), the volumetric and linear CTE can be obtained. The heat capacity can be also calculated based on the volumetric averaging using Eq. (3). The density of the REVs is calculated by Eq. (4). The results of all calculations for the HD and LD C-S-H are presented in Table 2 (those values written in the parenthesis). The obtained results are in a good agreement with the results presented by a recent study though an atomic modelling [9]. In that study, the volumetric CTE for C-S-H globules was reported as 45×10^{-6}, with no distinction between the HD and LD C-S-H. Based on the results in the present

study, the values of 45.39×10^{-6} and 54.12×10^{-6} are calculated for, respectively, the HD and LD C-S-H, which will be used later for the cement paste microstructure.

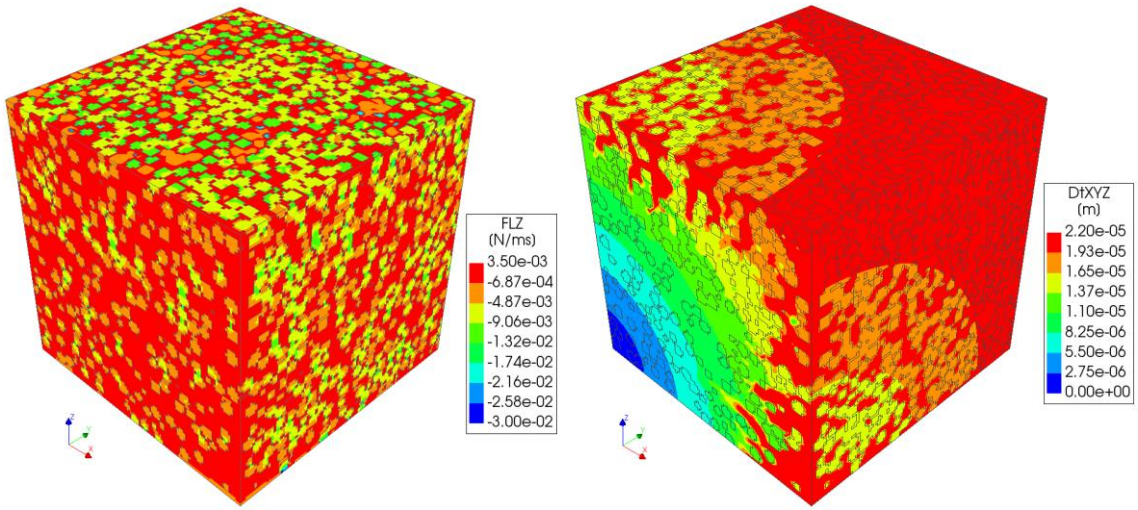

Figure 7. Results of heat flux in direction *z* (left), and results of maximum deformation field in three space directions (right) in the REV nanostructure of the outer C-S-H

4.2. Microscale

Microscale refers to the microstructure of cement paste, where the hydration products, cement grains and capillary pores are presented. The latest version of HYMOSTRUC3D software [8] is used for constructing the cement paste microstructure during hydration. This simulation is implemented in a cubic REV volume of the cement paste, where the cement particles are modelled as spheres randomly distributed. The initial number and diameter of the particles are built in accordance with the PSD curves for the cement clinker grains and for the limestone (non-reactant particles). These two curves were plotted in Figure 1. The main cement hydration products are the C-S-H and the Calcium Hydroxide (CH). C-S-H is formed as two layers of inner and outer products, which are the result of the inward and outward radial growing of the cement spheres. The inner layer refers to HD C-S-H, while the outer layer refers to LD C-S-H as described previously. The important parameters to be defined in HYMOSTRUC3D for modelling cement hydration are minimum and maximum size of the cement particles, REV size, temperature, w/c, and two reaction factors that control the speed and progress of hydration. For further details on fundamental aspects of the model parameters, the reader is addressed to the studies in [8, 9]. The hydration analysis was performed for w/c=0.62 as it is the water to cement ratio in the

concrete mix design in Table 3. The curing temperature was set at 20ºC. An image of the microstructure can be seen in Figure 8, with colour definition of different material phases.

Table 4. Main model hydration parameters in HYMOSTRUC3D

Dimensions the REV cube	100×100×100μm^3
Reactant	C3S, C2S, C3A, C4AF and gypsum
Product phases	Inner layer C-S-H; Outer layer C-S-H; CH grain; Limestone
Minimum and maximum particle size	1μm – 70μm
Temperature	20ºC
PSD parameters for cement clinker: b **,** n	0.052, 1.0 (see Figure 1)
PSD parameters for limestone: b **,** n	0.16, 2.0 (see Figure 1)
Hydration parameters: $k_0, d_{tr}, \beta_1, \beta_2$ *****	0.074, 3.0, 1.0, 1.0

* Details about these parameters are referred to study published by Van Breugel in 1995 [14].

A total number of 8 discretized REV microstructures of cement paste are constructed at 8 time steps of hydration, which are solved in DIANA FEA under a steady state heat transfer analysis and a linear structural analysis, as described in Section 3. The results from these two analyses are shown in Figure 9 for the microstructure of cement paste at the last time step corresponding to 360h of hydration, with a degree of reaction $\alpha = 0.85$. By using Eqs. (1), (3), (4), (7) and (10), the effective thermal conductivity (λ_{eff}), the effective specific heat capacity (C_{peff}), the density, the volumetric and linear CTE (α_T), and can be calculated respectively. It worth noticing that the results of microstructure corresponds to a saturated condition for the cement paste, where all capillary pores are assumed filled with water. Later in this study, the effect of losing water from the cement paste REV will be investigated. The results for all steps of analysis are written in Table 5, and plotted in Figure 10. These results are input properties for the mesoscale modelling of mortar.

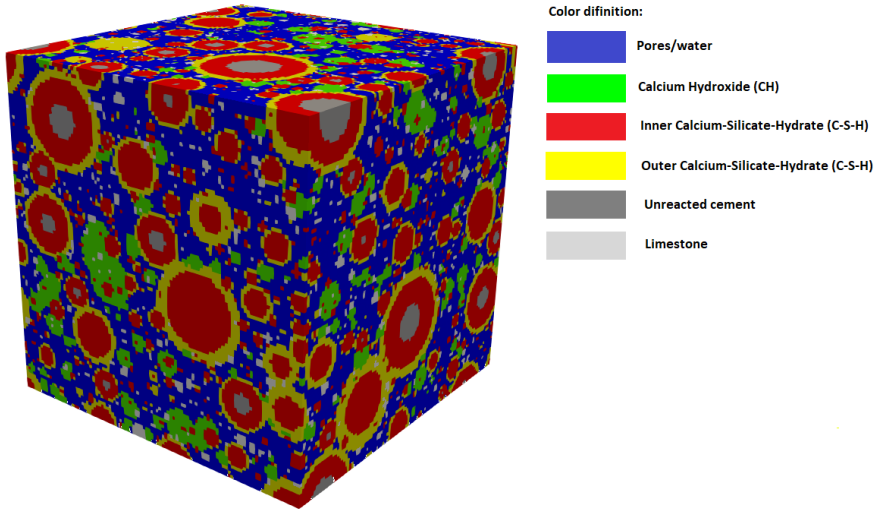

Figure 8. Microstructure of cement paste with w/c=0.62 at degree of reaction α=0.85

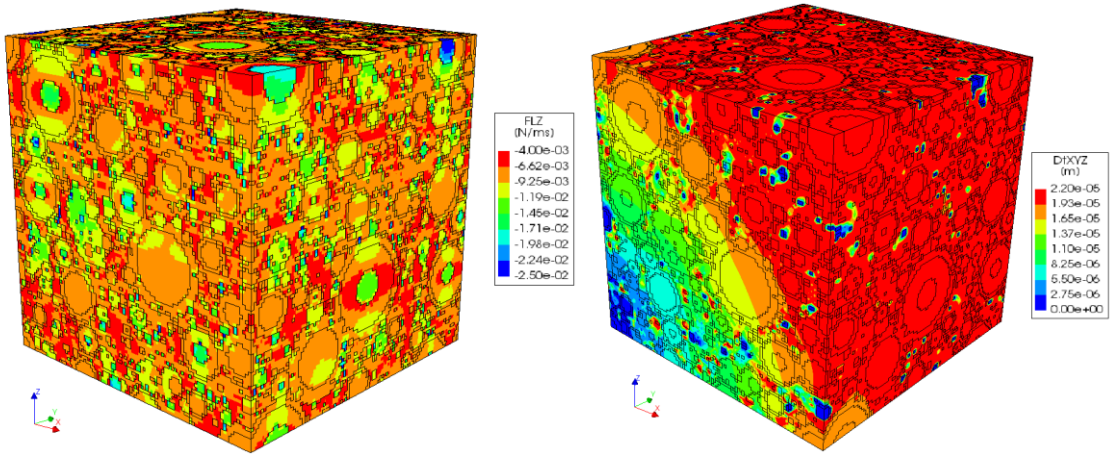

Figure 9. Results of heat flux in direction z (left), and results of maximum deformation field in he three space directions (right) in the REV macrostructure of cement paste at α=0.85

4.3. Mortar

Mesoscale refers to mortar, which is of the order 10^{-4} to 10^{-2}m. At this scale, the material phases are the porous cement paste matrix (microstructure), sand particles (ranging from 0.01-4mm in size), and Interfacial Transient Zone (ITZ) between sand particle's surface and cement matrix, which according to the literature ranged between 10-50μm in thickness [23-25]. In order to construct the mesostructure of REV for mortar, sand particles are assumed as spheres distributed into a cubic volume of 10x10x10mm^3. The size and distribution of the sand particles are based

on the PSD curve presented in Figure 2 for fine aggregates. Based on the theoretical volume calculated in the concrete mix design written in Table 3, the volume ratio between the fine aggregates and the cement paste matrix is about 1.35, in which the total volume of matrix and sand aggregates in the REV are about, respectively, 42% and 56%. Therefore, a total of 2% of REV mesostructure volume is occupied by air voids, which are simulated as “air spheres” ranging from 0.1 to 1mm in diameter.

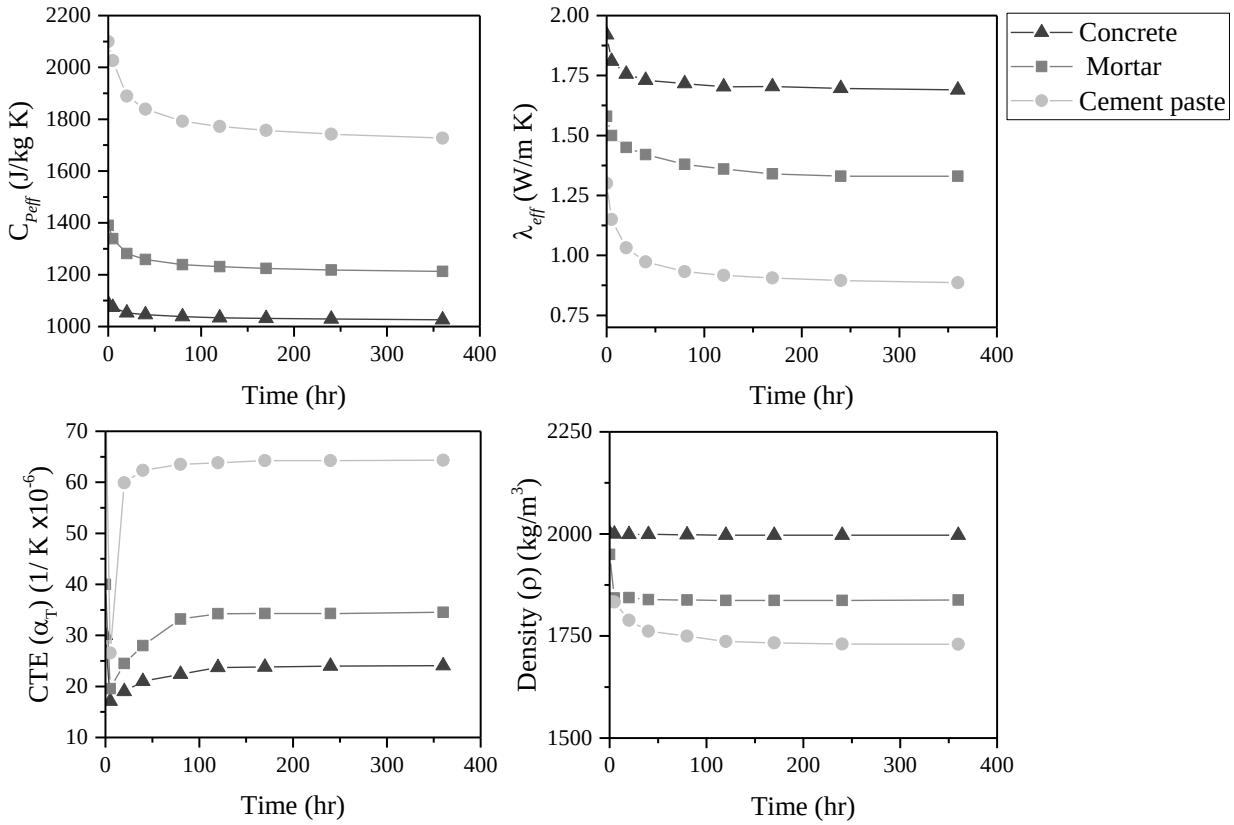

Figure 10. Evolution of the thermal properties and density of the cement paste, mortar and concrete during hydration for a saturated condition corresponding to the concrete mix design

The ITZ can be considered as the outer layer of sand spheres, which are becoming a volume part of the cement paste matrix. ITZ is normally considered as cement paste matrix with a high amount of porosity [2]. However, according to the literature the effect of ITZ on the physical properties of concrete (e.g. the thermal properties) is not significant [26, 27]. Hence, for the calculation of the thermal properties, the presence of ITZ material phases is neglected. Later in the parametric study section, the effect due to ITZ is investigated. The constructed REV is discretised by dividing the

length of the REV into 100 units, being each voxel with a size of 0.1x0.1x0.1mm^3. Therefore, the smallest size of fine aggregate that is presented in the REV is 0.1mm. The discretised REV mesostructure of mortar is illustrated in Figure 11. The colours distinguish the sand particles (dark grey) from the cement paste matrix (light grey). No voxel (or element) is constructed for the "air spheres", which can be seen in the figure.

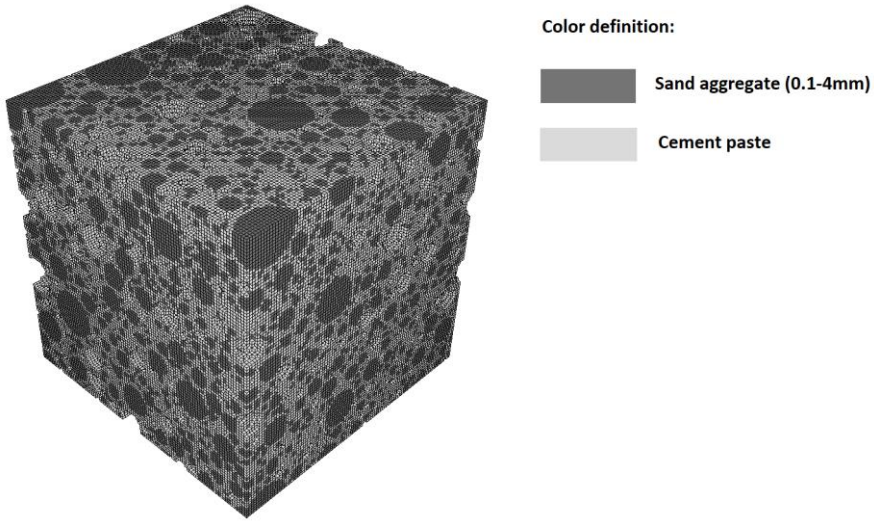

Figure 11. Mesostructure REV of 10x10x10mm^3 of the mortar

The discretized REV mesostructure of mortar is imported into in DIANA FEA and is solved under a steady state heat transfer analysis and a linear structural analysis as described in Section 3. The results from these two analyses are shown in Figure 12 for the mesostructure corresponding to cement paste properties at a degree of reaction α=0.85. By using Eqs. (1), (3), (4), (7) and (10) the effective thermal conductivity (λ_{eff}), the effective specific heat capacity (C_{peff}), the density, and the volumetric and linear CTE (α_T) can be calculated. By varying the properties of cement paste in accordance with hydration progress, the thermal properties of mortar can be calculated at each level of cement hydration as written in Table 5, and plotted in Figure 10. These results are input properties for the macroscale modelling of concrete.

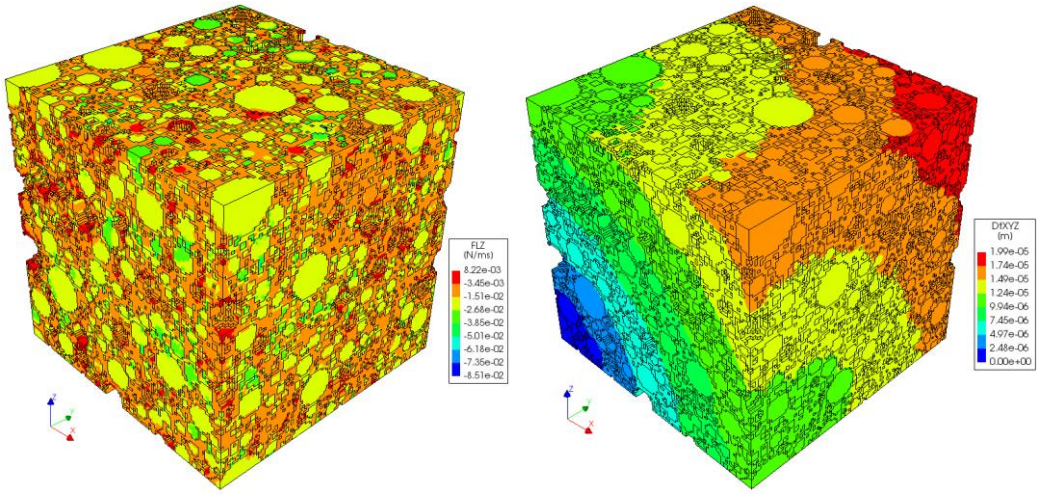

Figure 12. Results of heat flux in direction z (left), and results of maximum deformation field in three space directions (right) in the REV mesostructure of mortar corresponding to cement paste properties at α=0.85

4.4. Macroscale

Macroscale refers to concrete, which is of the order 10^{-2} to 1m. At this scale, the material phases are the porous mortar (mesostructure) and the coarse aggregates (bigger than 5mm in size). In order to construct the macrostructure of REV of concrete, coarse particle are assumed as spheres being distributed into a cubic volume of 100x100x100mm^3. The size and distribution of the coarse particles are based on the PSD curve presented in Figure 2. Based on the theoretical volume calculated in the concrete mix design written in Table 3, the volume ratio between the coarse aggregate and mortar is about 0.55, in which the total volume of mortar matrix and coarse aggregates in the REV are about, respectively, 64% and 35%. Therefore, a total of 1% of REV mesostructure volume is occupied by air voids, which are simulated as “air spheres” ranging from 1.1 to 15mm in diameter. The constructed REV is discretised by dividing the length of the REV into 100 units, being each voxel with a size of 1.0x1.0x1.0mm^3. The discretised REV macrostructure of concrete is shown in Figure 13. The colours distinguish the coarse particle voxels (dark grey) and mortar voxels (light grey). No voxel (or element) is constructed for the “air spheres”, which can be seen in the figure.

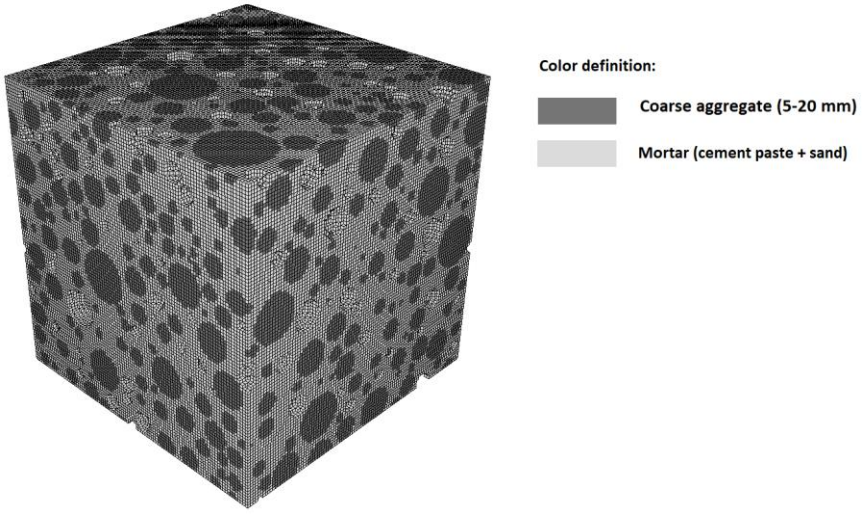

Figure 13. Macrostructure of the concrete REV of 100x100x100mm^3 including the coarse aggregates and the mortar

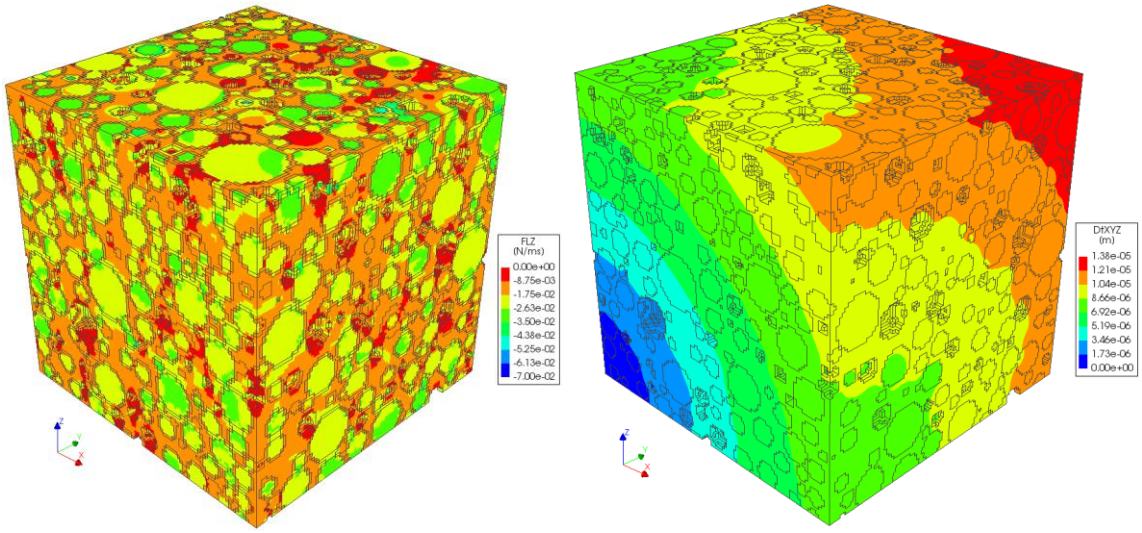

Figure 14. Results of heat flux in direction z (left), and results of maximum deformation field in three space directions (right) in the REV macrostructure of concrete corresponding to the mortar with cement paste matrix at α=0.85

The discretized REV macrostructure of concrete is solved in DIANA FEA under a steady state heat transfer analysis and a linear structural analysis as described in Section 3. The results are shown in Figure 14 for the macrostructure corresponding to mortar properties at a degree of reaction α=0.85 for the cement paste matrix. By using Eqs. (1), (3), (4), (7) and (10), the effective thermal conductivity (λ_{eff}), the effective specific heat capacity (C_{peff}), the density, and the

volumetric and linear CTE (α_T) can be calculated. By varying the properties of mortar the thermal properties of concrete can be calculated as written in Table 5, and plotted in Figure 10.

Table 5. Thermal properties obtained from the modelling for cement paste and mortar

	Time of hydration and Degree of reaction α (%)	Thermal Conductivity λ (W/m.K)	Specific heat capacity C_P J/(kg.K)	Thermal expansion coefficient (CTE) α_T ×10^{-6} (1/K)				Density ρ kg/m^3
				linear			volume	
				x	y	z		
Cement paste * (CEM IIA/L42.5R) w/c = 0.62	5 hr, α=7	1.150	2026	8.50	9.01	9.04	26.55	1717
	20 hr, α=39	1.032	1889	20.22	19.37	20.32	59.91	1719
	40 hr, α=57	0.973	1839	21.64	20.23	20.48	62.35	1709
	80 hr, α=70	0.932	1792	21.91	20.62	20.98	63.51	1706
	120 hr, α=75	0.917	1772	22.05	20.65	21.12	63.83	1705
	170 hr, α=78	0.906	1757	22.00	20.95	21.15	64.24	1705
	240 hr, α=82	0.895	1742	21.99	21.07	21.18	64.24	1705
	360 hr, α=85	0.886	1727	21.95	21.14	21.24	64.34	1706
Mortar ** w/c = 0.62	5 hr, α=7	1.50	1339	6.52	6.52	6.53	19.57	1843
	20 hr, α=39	1.45	1282	9.10	8.42	8.49	24.50	1844
	40 hr, α=57	1.42	1259	11.45	11.40	11.38	34.05	1839
	80 hr, α=70	1.40	1239	11.48	11.43	11.41	34.15	1838
	120 hr, α=75	1.38	1231	11.52	11.45	11.42	34.25	1837
	170 hr, α=78	1.34	1224	11.50	11.47	11.48	34.27	1837
	240 hr, α=82	1.33	1218	11.48	11.49	11.50	34.30	1837
	360 hr, α=85	1.33	1213	11.50	11.50	11.52	34.52	1838
Concrete * w/c = 0.62**	5 hr, α=7	1.81	1074	5.67	5.81	5.72	17.12	2000
	20 hr, α=39	1.76	1053	6.21	6.24	6.30	19.05	1999
	40 hr, α=57	1.73	1045	7.05	7.15	7.12	21.52	1999
	80 hr, α=70	1.72	1038	7.39	7.43	7.51	22.43	1998
	120 hr, α=75	1.70	1033	7.52	7.51	7.62	23.72	1997
	170 hr, α=78	1.70	1031	7.53	7.53	7.63	23.86	1997
	240 hr, α=82	1.69	1029	7.55	7.54	7.81	24.01	1997
	360 hr, α=85	1.69	1026	7.59	7.60	7.83	24.06	1997

* The values reported from modelling of the microstructure of cement paste during hydration;
** The values obtained from the mesoscale modelling of mortar with the same cement type;
*** The values obtained from the macroscale modelling of concrete with the same mortar and cement paste.

5. Validation of the model

Validation of the model will be made for the case of the specific heat capacity and the thermal conductivity. In Figure 15 the obtained numerical results in terms of the effective thermal conductivity are compared to the results from recent studies in the literature [7, 28-31] for w/c

ratios of 0.3 and 0.4, at different hydration times. It should be noted that the experimental results are collected only for saturated cement paste samples, and that the data is not necessarily correspondent to the same type of cement. Despite the observable scatter in the data obtained from the literature, the simulation lies within acceptable margins in regard to experimental data. In the same figure, a comparison is also made between the simulation results and some few data in the literature [7, 29, 32] in terms of the specific heat capacity per mass unit of cement paste. The specific heat capacity per unit mass is calculated in accordance with the density estimated with the model using the discretized REV microstructure. The measurement of thermal properties of the exact cement type simulated in the present paper is still an ongoing process, and cannot yet be communicated herein.

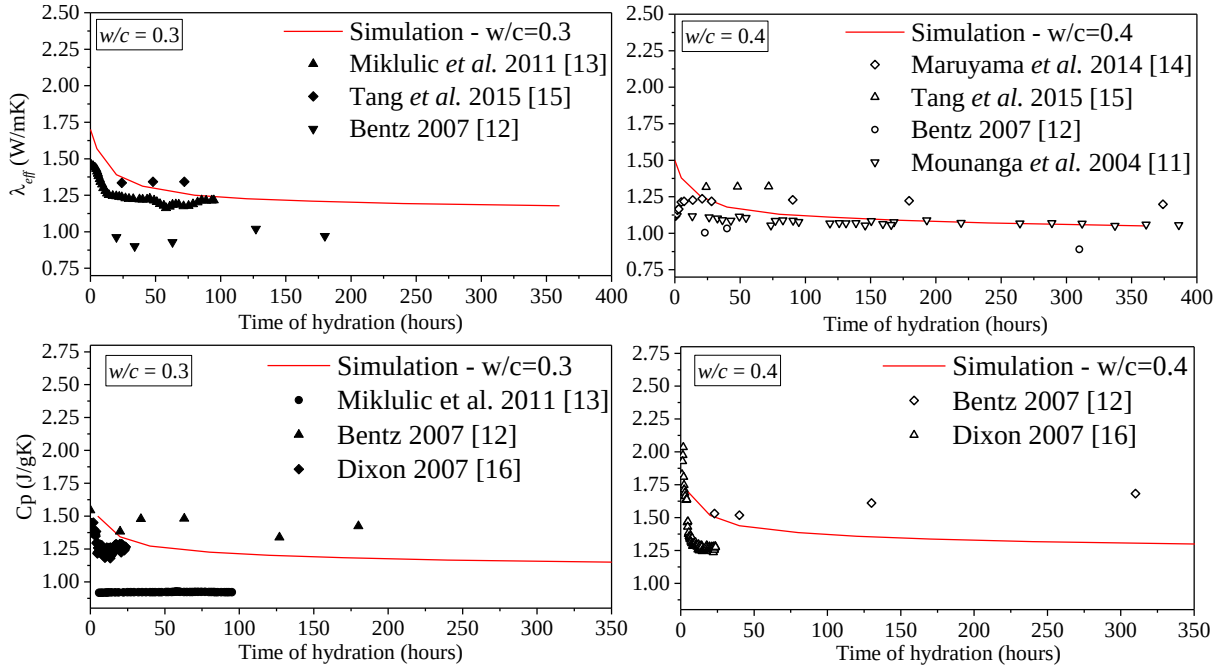

Figure 15. Comparison between the experimental and numerical results

6. Parametric study

With the aid of the multiscale numerical platform proposed in the previous sections, a parametric study is carried out hereafter in order to evaluate the effect of

1) water to cement ratio;

2) humidity (percentage of water content in porosity);

3) variation of cement paste properties;

4) Interfacial Transition Zone (ITZ) on the thermal properties of concrete

6.1. Effect of w/c

The effect of w/c ratio on the thermal properties of cement paste is plotted in Figure 16. While the specific heat capacity and the CTE increase by increasing w/c ratio, the thermal conductivity decreases. Both are in agreement with the experimental results from the literature [2]. The results in this section belong to the saturated condition. The change may be different when the dried cement paste is purposed for the simulation.

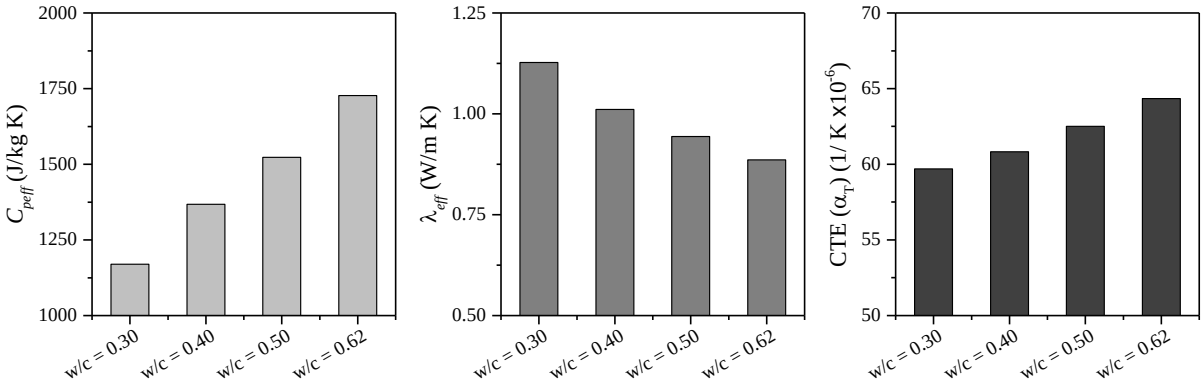

Figure 16. Effect of w/c on the effective thermal conductivity, on the specific heat capacity per unit mass, and on the volumetric CTE of cement pastes

6.2. Effect of humidity

One of the important aspects on measuring the thermal properties of the concrete is related to the humidity of the material, present in the porosity at different scales including gel water, inter-hydrate water and capillary water. In order to investigate the humidity effect on the thermal properties, four different levels of water content in the cement paste microstructure are investigated. For this purpose, a computer code is developed in order to randomly replace the pore voxels in the REV microstructure by empty spaces, representative of the water lost in the microstructure. This water loss continues until reaching a desired amount of humidity in the REV. For example, 25% humidity refers to the loss of 75% of the total water volume (or water mass) from the microstructure, meaning that the material properties of 75% of the pore voxels are changed by the properties of air for the steady state heat analysis, and the corresponding finite elements are thus eliminated for the structural analysis. Figure 17 shows, as an example, a slice of a cement paste microstructure with different levels of water content in the capillary porosity,

from fully saturated to fully dried microstructures. However, with this strategy only the loss of capillary water is presented. In reality, the loss of water occurs at the levels of both capillary and gel pores. In order to have a more realistic strategy, the same water loss strategy is implemented for the nanostructure of C-S-H, where the gel water is presented. Therefore, if the REV microstructure of cement paste loses 75% of its water at the capillary pore level, the C-S-H phases in this REV correspond to the nanostructure with 75% of water lost at gel pores for both HD C-S-H and LD C-S-H. The variation of the thermal properties of the nanostructure of HD C-S-H and LD C-S-H versus the humidity are plotted in Figure 18. These values are the input for the REV microstructure of the cement paste with different humidity levels. It is worth noticing that the specific heat capacity of both HD C-S-H and LD C-S-H reaches the same value 850J/kg.K^{-1} at 0% water content at gel pores. This proves the accuracy of the analysis because with no water, the model for both HD C-S-H and LD C-S-H has to present the same specific heat capacity of the C-S-H globules. The obtained value is very close the reported value of 840J/kg.K^{-1} for C-S-H globules (with Ca/Si=1.75) in the literature, as written in Table 2.

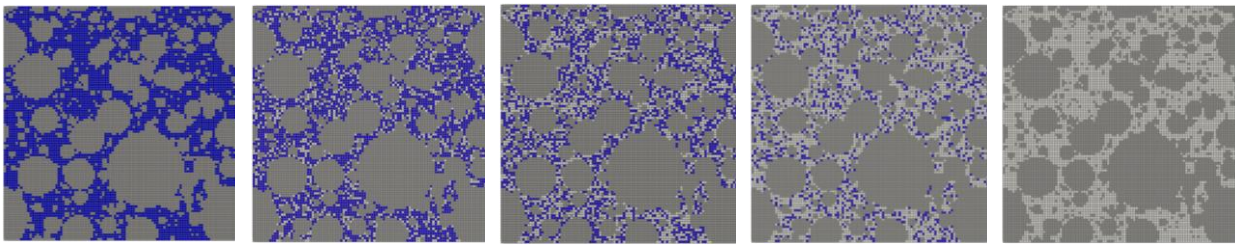

Fully saturated 25% dry 50% dry 75% dry Fully dry

Figure 17. Slice examples of cement paste microstructures from fully saturated to fully dried

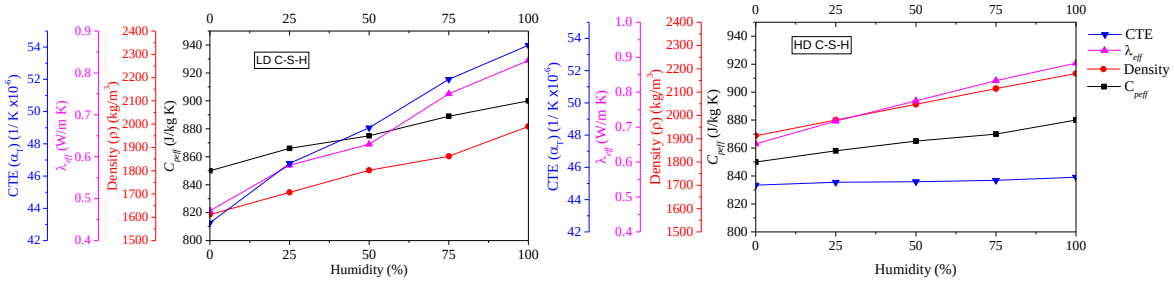

Figure 18. Variation of thermal properties of C-S-H hydration product by changing the percentage of water content

The variation of the thermal properties of the cement paste (with w/c=0.62) versus its humidity is plotted in Figure 19. All the thermal properties of the cement paste tend to decrease by decreasing

the humidity of the material. As it can be observed from the results, the thermal conductivity is the property that is most influenced. The effective thermal conductivity at fully dried samples decreases about 50% from its value at the saturated level. The decrease for the volumetric CTE, the density and the specific heat capacity are 14%, 30% and 41%, respectively. The decrease in the density can represent the total amount of porosity in the cement paste microstructure for w/c=0.62, as also obtained by HYMOSTRUC3D.

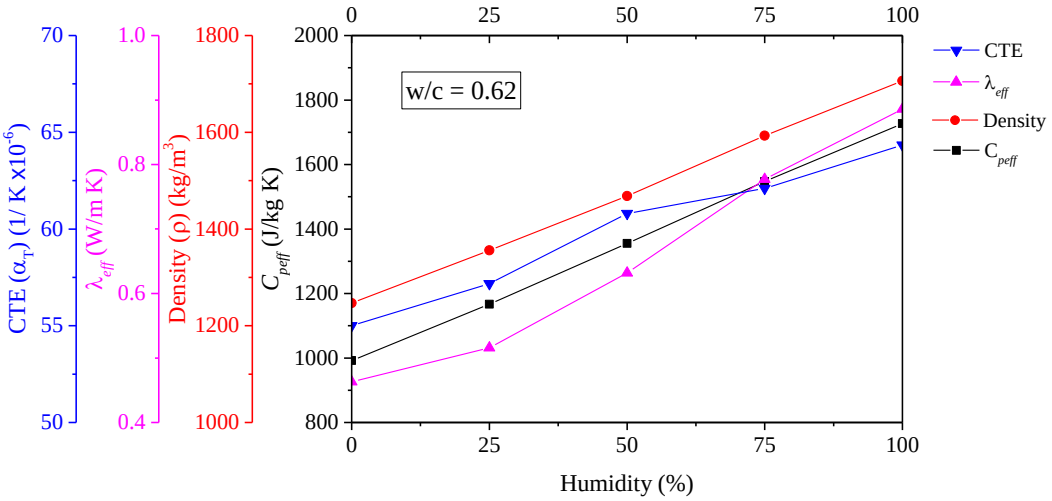

Figure 19. Variation of some thermal and physical properties of the cement paste by changing the percentage of water content

6.3. Effect of ITZ

According to the literature, thermal properties of concrete are not much influenced by the ITZ. The significant difference between the ITZ and the "core cement paste matrix" (the matrix in the space between fine aggregates) present in the mortar mesostructure is of about 5 to 10% in porosity. This may affect the mechanical properties, but not much the physical properties. In order to investigate this effect, the REV mortar mesostructure is constructed by considering a layer of ITZ at the outer surface of the fine aggregates. However, since the average reported thickness for ITZ is about 20μm [24, 26], the discretised REV mesostructure in Section 4.3 has to be refined. This requires each side of the REV to be divided into 500 units, in order to get the smallest voxel 0.02mm to be able to represent the ITZ thickness. This division gives 125x10^6 finite elements, which is practically impossible to be handled computationally. Therefore, the size of total REV mesostructure of mortar is decreased to 2x2x2mm^3. In this case, 100 unit divisions can represent

the ITZ thickness. However, the ITZ is limited to be associated to only those fine aggregates the size of which ranges from 0.1mm to 1mm. This REV is shown in Figure 20, where the ITZ around the fine aggregate spheres is represented in red colour.

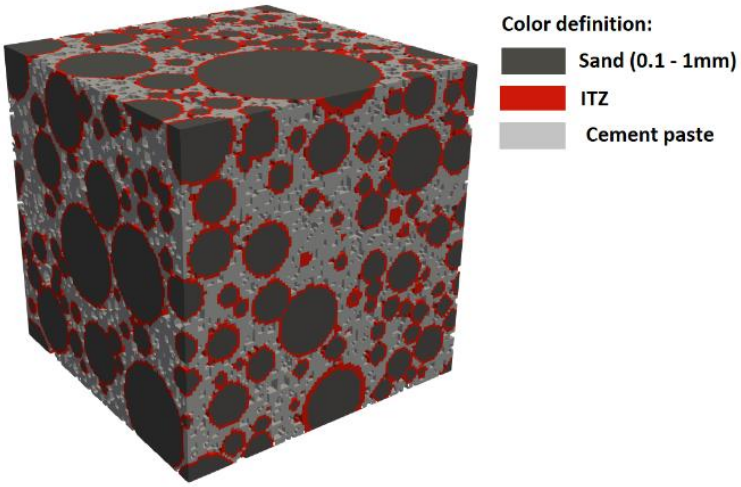

Figure 20. Mesoscale of a 2x2x2mm^3 REV of mortar, considering ITZ voxels around the sand ranging between 0.1mm and 1mm

The ITZ is usually considered as cement matrix with a higher amount of porosity [2], comparing with the core cement matrix. The definition of ITZ properties has to be defined based on relevant material tests. In the lack of data from such tests, and also with the intention to verify only the effect of ITZ on the thermal properties, the thermal properties of ITZ are defined as a percentage of the thermal properties of the cement paste matrix. For the thermal conductivity, ITZ is assumed to have a value ranging from 5 to 30% of the thermal properties of the cement paste matrix. For the specific heat capacity and CTE, ITZ is assumed with values ranging from 5 to 30% of the thermal properties of the cement paste matrix.

The discretized 2x2x2mm^3 REVs of mortar with ITZ material phases are solved in DIANA FEA under a steady state heat transfer analysis, and a linear structural analysis as described in Section 3. By using Eqs. (1), (3), (7) and (10), the effective thermal conductivity (λ_{eff}), the volumetric and linear CTE (α_T), and the effective specific heat capacity (C_{peff}) can be calculated. The variation of the thermal properties of the REV mesostructure of mortar is plotted versus the different ITZ thermal properties, which are the percentage of the thermal properties of cement paste matrix. The maximum variations in the thermal properties of mortar with 30% difference in the thermal

properties of ITZ and the cement paste matrix are 7.8%, 1.9% and 7% for, respectively, the specific heat capacity, the thermal conductivity and the volumetric CTE.

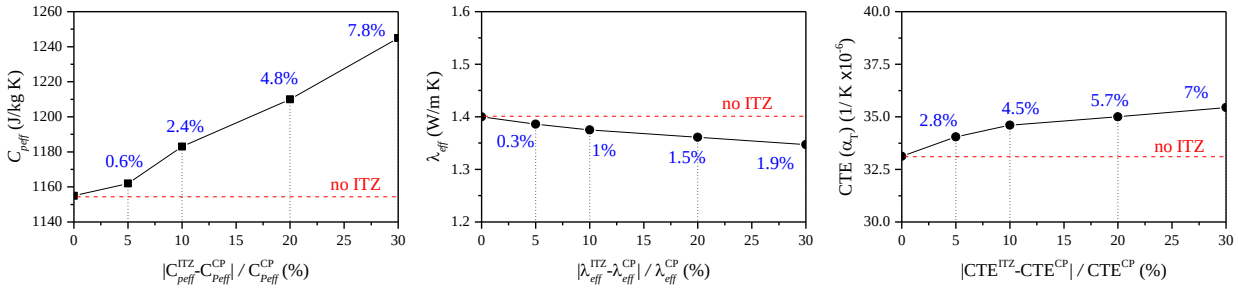

Figure 21. Variation of the thermal properties of mortar with and without considering the ITZ (superscript "CP" represents "Cement Paste")

6.4. Effect of variation of cement paste properties in concrete

Figure 22 illustrates how variations in cement paste thermal properties of 15% influence the estimations of the mortar and concrete thermal properties. In the cases studied here (especially with the volume fraction of aggregates adopted in the concrete mix design), incertitude of ±15% in the determination of the thermal properties of the cement paste induce variations of ±8.5% and ±4.5%, respectively, on the thermal conductivity of mortar and concrete. For the heat capacity, the variations in mortar and concrete are around ±9% and ±5%, respectively. For the volumetric CTE, the variations in mortar and concrete are of about ±11% and ±5%, respectively. These results suggest that even with the lack of data about the thermal properties of the cement paste constituents, a certain degree of confidence can be obtained in the estimations of concrete properties provided that the properties of aggregates are well controlled.

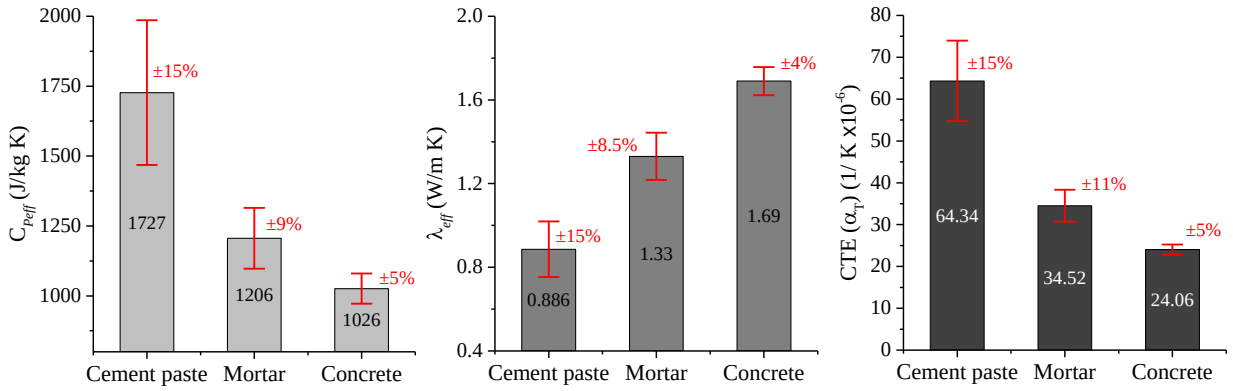

Figure 22. Variation of 15% in the thermal properties of cement paste on the thermal properties of mortar and concrete

7. Summary and conclusion

In this technical report, the thermal properties of concrete at early ages namely, the specific heat capacity, the thermal conductivity and the CTE, are estimated by means of a numerical homogenization tool that accounts for the material Representative Elementary Volume (REV), in combination of a multiscale definition of concrete at four different scales including: C-S-H nanostructure, cement paste microstructure, mortar mesostructure and finally macrostructure of concrete. Estimations of the thermal conductivity and specific heat capacity were in the range of the observed experimental results found in the literature, and decrease with the degree of hydration (or time). However, the CTE shows increasing tendency to reflect the growth of the degree of hydration. No validation is made in the present study for CTE. The conductivity decreases with the w/c, while the specific heat capacity and the CTE increases. All the thermal properties are sensitive to the amount of humidity in the material, and showed a decreasing trend by losing water from the microstructure of cement paste. This is much pronounced for the thermal conductivity, which shows a 50% decrease in fully dried conditions. The lowest effect of humidity was observed for the CTE, which decreased by only 14% in fully dried conditions.

Only small differences are observed in the estimations of the thermal properties of mortar and concrete in scenarios accounting for, or neglecting, the ITZ. The evaluation was made for a specific concrete mix design present in this study. Future research is needed to better define the ITZ characteristics, as well as its role on the thermal properties of mortar and concrete.

Further effort needs to be undertaken to validate in a more comprehensive and suitable way the modelling approach developed here, using a more exhaustive experimental campaign.

8. References

[1] Miguel Azenha, Rodrigo Lameiras, Christoph de Sousa, and Joaquim Barros, *Application of air cooled pipes for reduction of early age cracking risk in a massive RC wall.* Engineering Structures, 2014. **62-63**: p. 148-163.

[2] Tulio Honorio, Benoit Bary, and Farid Benboudjema, *Thermal properties of cement-based materials: Multiscale estimations at early-age.* Cement and Concrete Composites, 2018. **87**: p. 205-219.

[3] Paolo Morabito, *Thermal properties of concrete: variations with the temperature and during the hydration phase.* Milan, Italy: Department of Civil & Mining Engineering &Division of Structural Engineering, 2001.

[4] A. L. Marshall, *The thermal properties of concrete.* Building Science, 1972. **7**(3): p. 167-174.

[5] Cruz C. R. and Gillen M., *Thermal expansion of Portland cement paste, mortar and concrete at high temperatures.* Fire and Materials, 1980. **4**(2): p. 66-70.

[6] David G Cahill, Susan K Watson, and Robert O Pohl, *Lower limit to the thermal conductivity of disordered crystals.* Physical Review B, 1992. **46**(10): p. 6131.

[7] DP Bentz, *Transient plane source measurements of the thermal properties of hydrating cement pastes.* Materials and Structures, 2007. **40**(10): p. 1073.

[8] P. Acker, *Swelling, shrinkage and creep: a mechanical approach to cement hydration.* Materials and Structures, 2004. **37**(4): p. 237-243.

[9] Mohammad Javad Abdolhosseini Qomi, Franz-Josef Ulm, and Roland J. M. Pellenq, *Physical Origins of Thermal Properties of Cement Paste.* Physical Review Applied, 2015. **3**(6): p. 064010.

[10] Josephus Thomas Jr, Robert R Frost, and Richard D Harvey, *Thermal conductivity of carbonate rocks.* Engineering Geology, 1973. **7**(1): p. 3-12.

[11] Frank M. Etzler and Pamela J. White, *The heat capacity of water in silica pores.* Journal of Colloid and Interface Science, 1987. **120**(1): p. 94-99.

[12] Patrick A Bonnaud, Hegoi Manzano, Ryuji Miura, Ai Suzuki, Naoto Miyamoto, Nozomu Hatakeyama, and Akira Miyamoto, *Temperature dependence of nanoconfined water properties: application to cementitious materials.* The Journal of Physical Chemistry C, 2016. **120**(21): p. 11465-11480.

[13] Walter H Johnson and Willard H Parsons, *Thermal expansion of concrete aggregate materials*. 1944: US Government Printing Office.

[14] Klaas Van Breugel, *Numerical simulation of hydration and microstructural development in hardening cement-based materials:(II) applications.* Cement and Concrete Research, 1995. **25**(3): p. 522-530.

[15] Guang Ye, *Experimental study and numerical simulation of the development of the microstructure and permeability of cementitious materials*. 2003: PhD Thesis. TU Delft, Delft University of Technology.
[16] Shashank Bishnoi and Karen L Scrivener, *μic: A new platform for modelling the hydration of cements.* Cement and Concrete Research, 2009. **39**(4): p. 266-274.
[17] *Element Library*, in *DIANA-10.1 User's Manual*, J. Manie, Editor., DIANA FEA.
[18] R.A. Schapery, *Thermal Expansion Coefficients of Composite Materials Based on Energy Principles.* Journal of Composite Materials, 1968. **2**(3): p. 380-404.
[19] Mingzhong Zhang, *Multiscale lattice Boltzmann-finite element modelling of transport properties in cement-based materials*. 2013: TU Delft, Delft University of Technology.
[20] Thomas Y Hou and Xiao-Hui Wu, *A multiscale finite element method for elliptic problems in composite materials and porous media.* Journal of computational physics, 1997. **134**(1): p. 169-189.
[21] Salvatore Torquato, Thomas M Truskett, and Pablo G Debenedetti, *Is random close packing of spheres well defined?* Physical review letters, 2000. **84**(10): p. 2064.
[22] Monica Skoge, Aleksandar Donev, Frank H. Stillinger, and Salvatore Torquato, *Packing hyperspheres in high-dimensional Euclidean spaces.* Physical Review E, 2006. **74**(4): p. 041127.
[23] JP Ollivier, JC Maso, and B Bourdette, *Interfacial transition zone in concrete.* Advanced Cement Based Materials, 1995. **2**(1): p. 30-38.
[24] Sidney Diamond and Jingdong Huang, *The ITZ in concrete–a different view based on image analysis and SEM observations.* Cement and concrete composites, 2001. **23**(2-3): p. 179-188.
[25] Jing Hu and Piet Stroeven, *Properties of the interfacial transition zone in model concrete.* Interface Science, 2004. **12**(4): p. 389-397.
[26] Karen L Scrivener, Alison K Crumbie, and Peter Laugesen, *The interfacial transition zone (ITZ) between cement paste and aggregate in concrete.* Interface science, 2004. **12**(4): p. 411-421.
[27] JJ Zheng, CQ Li, and XZ Zhou, *Thickness of interfacial transition zone and cement content profiles around aggregates.* Magazine of Concrete Research, 2005. **57**(7): p. 397-406.
[28] Pierre Mounanga, Abdelhafid Khelidj, and Guy Bastian, *Experimental study and modelling approaches for the thermal conductivity evolution of hydrating cement paste.* Advances in cement research, 2004. **16**(3): p. 95-103.
[29] Dunja Mikulić, Bojan Milovanović, and Ivan Gabrijel, *Analysis of thermal properties of cement paste during setting and hardening*, in *Nondestructive Testing of Materials and Structures*. Springer. p. 465-471. 2013.

[30] Ippei Maruyama and Go Igarashi, *Cement reaction and resultant physical properties of cement paste.* Journal of Advanced Concrete Technology, 2014. **12**(6): p. 200-213.

[31] S. W. Tang, E. Chen, H. Y. Shao, and Z. J. Li, *A fractal approach to determine thermal conductivity in cement pastes.* Construction and Building Materials, 2015. **74**: p. 73-82.

[32] John C Dixon, *The shock absorber handbook*. 2008: John Wiley & Sons.